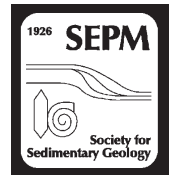


Journal of Sedimentary Research

Journal of Sedimentary Research, 2012, v. 82, 889–898
Current Ripples
DOI: 10.2110/jsr.2012.73



QUANTIFYING THE HIERARCHICAL ORGANIZATION OF COMPENSATION IN SUBMARINE FANS USING SURFACE STATISTICS

KYLE M. STRAUB¹ AND DAVID R. PYLES²

¹Department of Earth and Environmental Sciences, Tulane University, New Orleans, Louisiana 70118, U.S.A.

²Chevron Center of Research Excellence, Department of Geological Engineering, Colorado School of Mines, Golden, Colorado 80401, U.S.A.

e-mail: kmstraub@tulane.edu

ABSTRACT: Stratigraphy is often interpreted within hierarchical, or scale-dependent, frameworks that subdivide deposits based on distinct jumps in characteristics such as duration of deposition or scale. While the interpretation is logically valid, few studies quantitatively demonstrate that the jumps exist. Rather, recent work has quantitatively shown some characteristics of stratigraphy to be fractal, or scale invariant. Compensational stacking, the tendency for sediment-transport systems to preferentially fill topographic lows, is a concept widely used in stratigraphic interpretation. Here we use the compensation index, a metric that quantifies the strength of compensational stacking in sedimentary deposits, to describe the architecture of stratigraphy exposed in outcrops of submarine-fan strata in the Carboniferous Ross Sandstone representing contrasting architectural styles: (1) predominantly lobe elements and (2) predominantly channel elements. In both datasets, the stratigraphic architecture is classified into hierarchical classes of beds, stories, and elements. Results are the following. First, at both sites we document statistically significant increases in the strength of compensation across larger hierarchical levels supporting the use of hierarchical interpretations of stratigraphy. It is therefore plausible for some characteristics of sedimentary systems to be hierarchical and others to be fractal. Second, we document that lobe elements stack more compensationally than channel elements. We interpret this pattern to document that compensation increases along a longitudinal transect through this distributive submarine fan.

INTRODUCTION

Throughout history humans have classified naturally occurring phenomena into hierarchical, or scale-dependent, structures (e.g., phylogeny, Darwin 1861; human needs Maslow 1943) and engineered hierarchy into virtually every aspect of our lives (e.g., governments, roadways, computer networks). It is therefore no surprise that stratigraphers, in an effort to link stratigraphic architecture to depositional processes, subdivide the stratigraphic record into hierarchical units ranging in scale from laminae (Campbell 1967) to entire basin-fill successions (Mitchum et al. 1976). These classifications are based on distinct jumps, or scale-dependent changes, in characteristics such as duration of deposition, size, number of crosscutting relationships, and number of superimposed stratal bodies across hierarchical levels. Of particular importance to those studying landscape evolution and reservoir architecture are the mesoscale units, which we define as those larger than the lamina–laminaset hierarchy of Campbell (1967) and smaller than systems tracts of Brown and Fisher (1977). Several competing classification schemes exist for mesoscale units in submarine settings (e.g., Mutti and Normark 1987; Gardner and Borer 2000; Pyles 2007; Deptuck et al. 2008; Prelat et al. 2009; Prelat et al. 2010). While there are important differences between the schemes, all utilize similar descriptive components, including nature of bounding surfaces, external form, internal lithofacies distributions, and stacking patterns, which define units having either descriptive or interpreted genetic significance (Prather et al. 2000). Debate exists with regard to the underlying cause of hierarchy in

stratigraphy, with some arguing that it develops from cyclicity in boundary conditions that operate over a range of timescales (Einsele et al. 1991), while others argue that it develops from autogenic processes operating over a range of timescales (Royal and Sheets 2009).

With the exception of duration of deposition (Jackson 1975), scale (e.g., Gardner and Borer 2000; Pyles 2007; Deptuck et al. 2008; Pyles et al. 2010) and organic richness (Sageman et al. 1998), few studies quantitatively demonstrate that characteristics change across hierarchical levels. In a critical review of the largely interpretive and qualitative nature of hierarchical models, Schlager (2004) used shape analysis of clinoforms of varying scale to demonstrate a fractal, or scale-invariant, pattern. As fractal and hierarchical order are mutually exclusive conditions, Schlager (2004, p. 195) concludes orders of hierarchy “seem to be subdivisions of convenience rather than an indication of natural structure” and recommends future work to focus on a disciplined statistical characterization of spatially varying units. Schlager (2010) further demonstrates a scale-invariant pattern when sedimentation rates, rates of change of accommodation, and the power of sea-level changes are compared to observation span.

Compensational stacking is the tendency of deposits to preferentially fill topographic lows, smoothing out topographic relief by “compensating” for the localized deposition of discrete units. This tendency is interpreted to result from reorganization (i.e., avulsion) of the sediment-transport field to minimize potential energy associated with elevation gradients (Mutti and Normark 1987; Stow and Johansson 2000). Early models by Mutti and Sonnino (1981) and Mutti and Normark (1987)

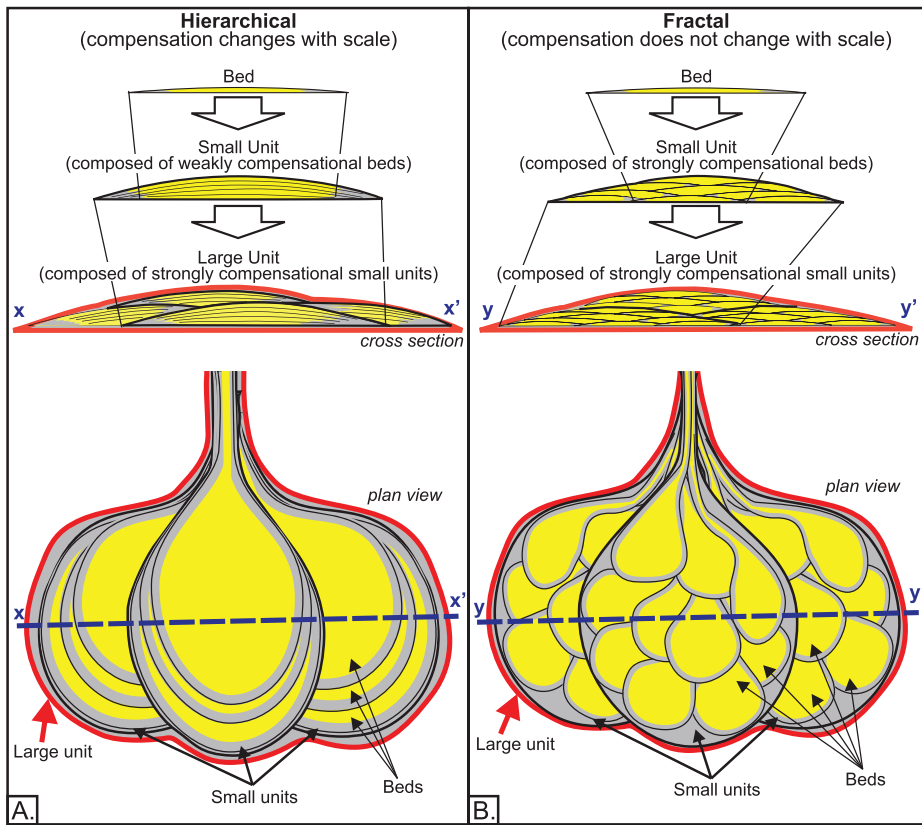


FIG. 1.—**A**) Diagram of hierarchical, scale-dependent, compensation whereby large units stack more compensationally than small units (no scale implied). Yellow represents sand-rich strata and gray represents mud-rich strata. **B**) Diagram of fractal, scale-invariant, compensation whereby compensation does not change with scale.

describe depositional units resulting from compensational stacking. They interpret these units to record sediment-transport fields fixed over short time intervals, resulting in lenticular deposits with positive surface relief. The boundaries between units are interpreted to record avulsions which redirect the sediment-transport field to local topographic lows. This interpretation qualitatively supports a hierarchical, or scale-dependant, organization to compensation. A diagram of hierarchical compensation is shown in Figure 1A. In contrast, Deptuck et al. (2008) used high-frequency seismic data to interpret a distributary channel-lobe system offshore Corsica. They interpret the geometry and stacking of small-scale units to mimic that of large-scale units so a lobe can be constructed of equally compensational units over multiple spatial scales (see their figure 17). This interpretation is shared by Prelat et al. (2010, their figure 2). Although hierarchical terms are used by these authors, their interpretations and diagrams support a fractal or scale-invariant organization to compensation. A diagram of fractal compensation is shown in Figure 1B.

Recently, Straub et al. (2009) developed the compensation index, a metric that quantifies the degree of compensation in sedimentary deposits by comparing observed stacking patterns to simple, uncorrelated stacking. This method uses the rate of decay of spatial variability in sedimentation between picked depositional horizons with increasing vertical stratigraphic scale. This approach allows identification of specific time and space scales relevant to stratigraphic architecture (Wang et al. 2011).

In this paper, we examine for the first time the mesoscale architecture of submarine stratigraphy in superbly exposed outcrops with a modified version of the compensation index to test for statistically significant differences in the strength of compensation between deposits of varying scale when classified in a hierarchical framework. Additionally, we examine how strength of compensation varies between predominantly channelized and predominantly unchannelized submarine settings in each hierarchical class in order to test how compensation varies spatially in submarine fans.

Submarine-fan deposits are ideal for this type of analysis due to the strongly aggradational nature of the morphological evolution relative to more progradational settings (i.e., deltaic deposits). The high degree of aggradation and strongly depositional nature of flows results in thick deposits with discrete individual surfaces that can be traced over long distances, rather than being repeatedly dissected by later deposits (Normark et al. 1979; Peakall et al. 2000; Macdonald et al. 2011). In addition, submarine fans occupy a critical place as the terminal sink in source–sink transport systems and host many large producing petroleum reservoirs (Weimer and Link 1991).

GEOLOGICAL SETTING

The Carboniferous Ross Sandstone crops out on sea-cliff exposures of Loop Head Peninsula, western Ireland (Fig. 2). The formation was deposited in the actively subsiding Carboniferous Shannon Basin (Martinsen et al. 2003; Pyles 2008). The Ross is one of four siliciclastic lithostratigraphic units that fill the basin (Fig. 2). Rider (1974) used trace fossils, lithofacies, stacking patterns, and stratal architecture to interpret the Ross Sandstone as sand-rich turbidites deposited in a submarine fan. Later work by Collinson et al. (1991), Chapin et al. (1994), Elliott (2000), Martinsen et al. (2000), Sullivan et al. (2000), Wignall and Best (2000), Lien et al. (2003), Martinsen et al. (2003); Pyles (2007, 2008), Pyles and Jennette (2009), Pyles et al. (2011), and Macdonald et al. (2011) support this interpretation.

DATA AND METHODOLOGY

The Ross Sandstone is notable for having some of Earth's best exposed and most laterally persistent outcrops of submarine-fan deposits. Two exceptionally well exposed outcrops, representing distinctive architectural styles, are located on the southern coast of Loop Head Peninsula (Fig. 2):

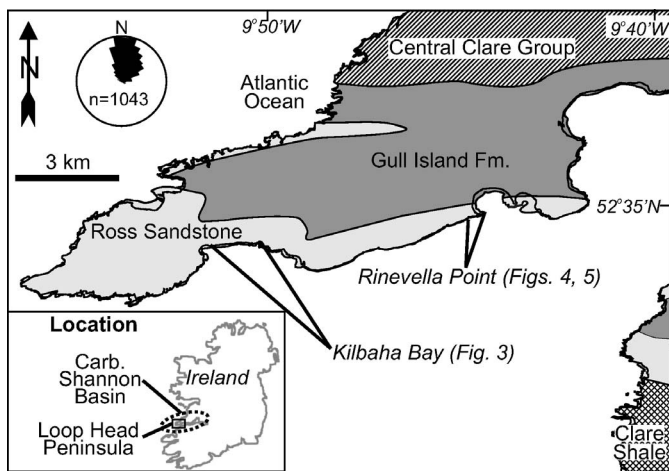


FIG. 2.—Geologic map of Loop Head Peninsula, County Clare, Ireland. The Ross Sandstone crops out on coastal exposures around the perimeter of the peninsula. The rose diagram represents paleocurrent measurements collected from flutes, grooves, ripples, and channel-margin orientations at all stratigraphic positions and from all parts of the outcrop belt, revealing a modal sediment transport direction to the north. Map and rose diagram are modified from Pyles (Pyles 2008).

(1) Kilbaha Bay and (2) Rinevella Point. Kilbaha Bay contains strata from the middle Ross Sandstone whereas Rinevella Point contains strata from the lower part of the upper Ross Sandstone (Pyles 2008). Figures 3 and 4 contain depositional-strike-oriented correlation panels and photographs of the exposures. The correlation panels were constructed by correlating, through direct observation, all mappable stratigraphic surfaces between closely spaced (9 to 28 m) stratigraphic columns. The columns document stratal boundaries, physical sedimentary structures, and grain size at 2 cm resolution.

Two types of architectural elements are recognized in the studied outcrops: (1) lobe elements and (2) channel elements. The terminology used herein is similar to that used for channel deposits by Gardner and Borer (2000), Pyles (2007), and Pyles et al. (2010) and for lobe deposits by Ghiaurov (1980), Pyles (2007), Pyles and Jennette (2009), Deptuck et al. (2008), Prelat et al. (2009), Prelat et al. (2010), and Macdonald et al. (2011).

Lobe elements contain flat to weakly erosional lower bounding surfaces and planar to broadly convex-upward upper bounding surfaces (Figs. 3, 5). Erosion is related to megaflutes, and the location of the maximum amount of erosion underlies the axis, the thickest part, of the element (Fig. 3C). In contrast to channel elements, the amount of erosion in lobe elements does not scale to the thickness of the element. Lobe elements contain distinctive upward and axis-to-margin changes in lithofacies (Figs. 3, 5). The axes, or thickest part, of lobe elements most commonly contain thickening- and coarsening-upward successions of beds that commonly locally overlie megaflutes, with the lower beds containing interbedded, thin-bedded, laminated shale with thin-bedded sandstone that are overlain by interbedded, thin-bedded sandstone with laminate shale, which are in turn overlain by thick-bedded, amalgamated, structureless sandstone and to a lesser degree structureless sandstone with shale clasts, and planar-laminated sandstone. The thick, amalgamated beds in the upper, axial parts of lobe elements laterally become thinner, deamalgamate, and transition into thin-bedded sandstone with laminated shale and eventually laminated shale with thin-bedded sandstone toward the margins of the lobe element. Pyles (2007) measured the dimensions of all well exposed lobe elements in the Ross Sandstone and calculated an average thickness of 2 m and an average aspect ratio of 1100:1. Kilbaha Bay contains predominantly lobe elements (Fig. 3).

Lien et al. (2003) interpret these tabular units as splays that resulted from gravity currents spilling laterally out of channels at sharp bends. We favor the lobe interpretation, because the units: (1) have sediment transport directions similar to those of stratigraphically adjacent channel elements, (2) are similar in thickness to channel elements (Pyles 2007), (3) have the same grain-size distributions as channel elements (Fig. 3), (4) are an order of magnitude greater in proportion than channel elements (Pyles 2008), and (5) display all of the characteristics described for lobe elements elsewhere in the Ross Sandstone where channel elements are not present, such as at Kilcloher Cliff and Dunmore Head (Pyles 2008), and at Ross Bay (Macdonald et al. 2011).

Channel elements contain erosional, concave-upward lower bounding surfaces and planar upper bounding surfaces except where they are locally eroded (Fig. 4). The amount of erosion scales to the thickness of the element. Channel elements contain distinctive axis-to-margin changes in lithofacies (Figs. 3, 5). The axes, or thickest parts, of channel elements commonly contain a lower shale-clast conglomerate overlain by thick-bedded, amalgamated, structureless sandstone and to a lesser degree structureless sandstone with shale clasts and large-scale cross-stratified sandstone. These beds laterally thin, deamalgamate, and transition to thin-bedded sandstone with laminated shale and laminated shale with thin-bedded sandstone toward the margin. Surfaces within channel elements are commonly locally erosional. Pyles (2007) measured the dimensions of all well exposed channel elements in the Ross Sandstone and calculated an average thickness of 4 m and an average aspect ratio of ~ 60:1. Rinevella Point contains predominantly channel elements (Fig. 4).

In an effort to unify hierarchical designations for channels and lobes we apply a common three-level hierarchy based on the Pyles (2007) hierarchical classification for channels in the Ross Sandstone (Figs. 3, 4): (1) bed, (2) story, and (3) element. The hierarchical terms are used as modifiers to the architectural style (e.g., channel story, channel element). Table 1 compares the hierarchical terms used herein with those of selected other studies. A bed is interpreted to be the product of a single depositional event (Campbell 1967), such as a turbidite resulting from a turbidity current. Photographic and diagrammatic examples of beds are shown in Figure 5. The correlation panels document beds to cluster into larger units whereby all beds in the larger units have similar lithofacies associations and the location of the axes, or thickest part, of vertically adjacent beds are superimposed. At this location, the boundaries between beds are commonly amalgamated, meaning that sandstone in adjacent beds is juxtaposed due to centimeter-scale erosion. Lateral to this site, beds are separated by shale laminae. Successive beds become thicker and coarser grained in an upward transect through the unit. Following the work of Friend et al. (1979), we refer to these units as stories. Photographic and diagrammatic examples of stories are shown in Figure 5.

Figures 3, 4, and 5 document stories grouping into larger units whereby all the stories in the larger unit have similar lithofacies associations, and the location of the axes of vertically adjacent stories are nearly superimposed (Fig. 5). At this location the boundaries between stories are commonly amalgamated due to decimeter-scale erosion. Lateral to this site, stories are separated by shale beds. Successive stories become thicker and coarser grained in an upward transect through the larger unit (Fig. 5). Following the work of Pyles (2007) for channels in the Ross Sandstone and Macdonald et al. (2011) for lobes in the Ross Sandstone, we refer to these units as elements. Photographic and diagrammatic examples of elements are shown in Figure 5. The boundaries between stratigraphically adjacent elements record abrupt and relatively large-scale changes in (1) the location of the axes of the elements, (2) lithofacies, (3) bedding style, and (4) paleocurrent direction (Figs. 3, 4). Other studies such as Gardner and Borer (2000), Pyles (2007), Deptuck et al. (2008), Prelat et al. (2009), and Pyles et al. (2010) document a larger hierarchical

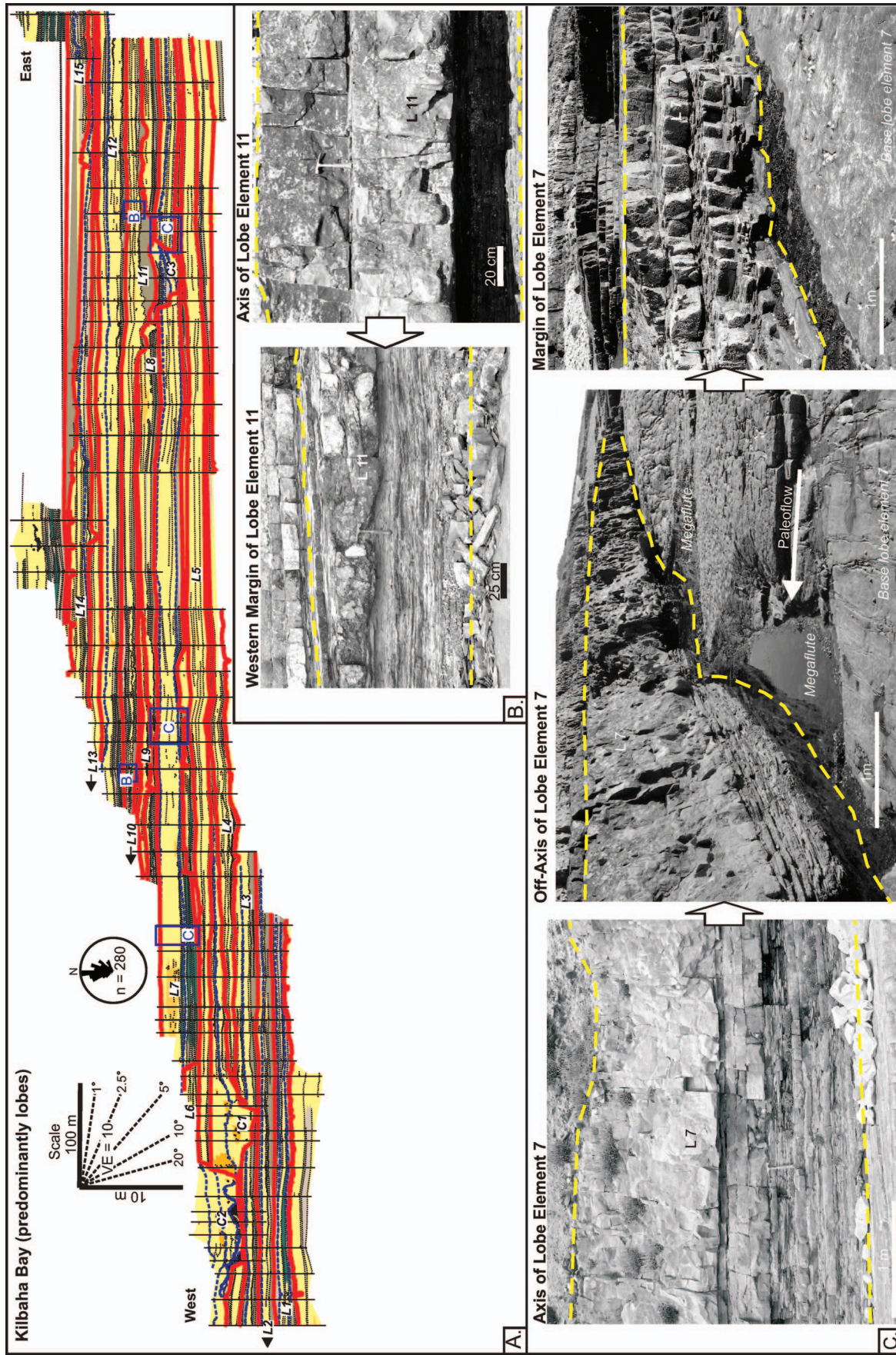


FIG. 3.—A) Correlation panel of the Kilbaha Bay outcrop. The location of the outcrop is labeled in Figure 2. The outcrop is ~ 1300 m wide and 30 m thick. Strata at the exposure dip ~ 5° north. Several small-offset strike-slip faults, where offset is less than the thickness of the exposure, are located in the outcrop and strata can be correlated across them with ease. The modal paleocurrent direction measured from flutes, grooves, ripples, and channel-margin orientations is 355°. The outcrop is oriented normal to this direction and is therefore a strike profile through the succession. The outcrop contains 15 lobe elements and three channel elements comprising ~ 95% and ~ 5% of the cross-sectional area of the exposure, respectively. Modified from Pyles (2004). Explanation of symbols used in correlation panel is included in Figure 4A. B, C) Photographs documenting axis-to-margin and upward changes in the stratigraphy of lobe element 11 and lobe element 7. Locations of photos are labeled in Part A. The upper and lower boundaries of the elements are labeled with yellow dashed lines.

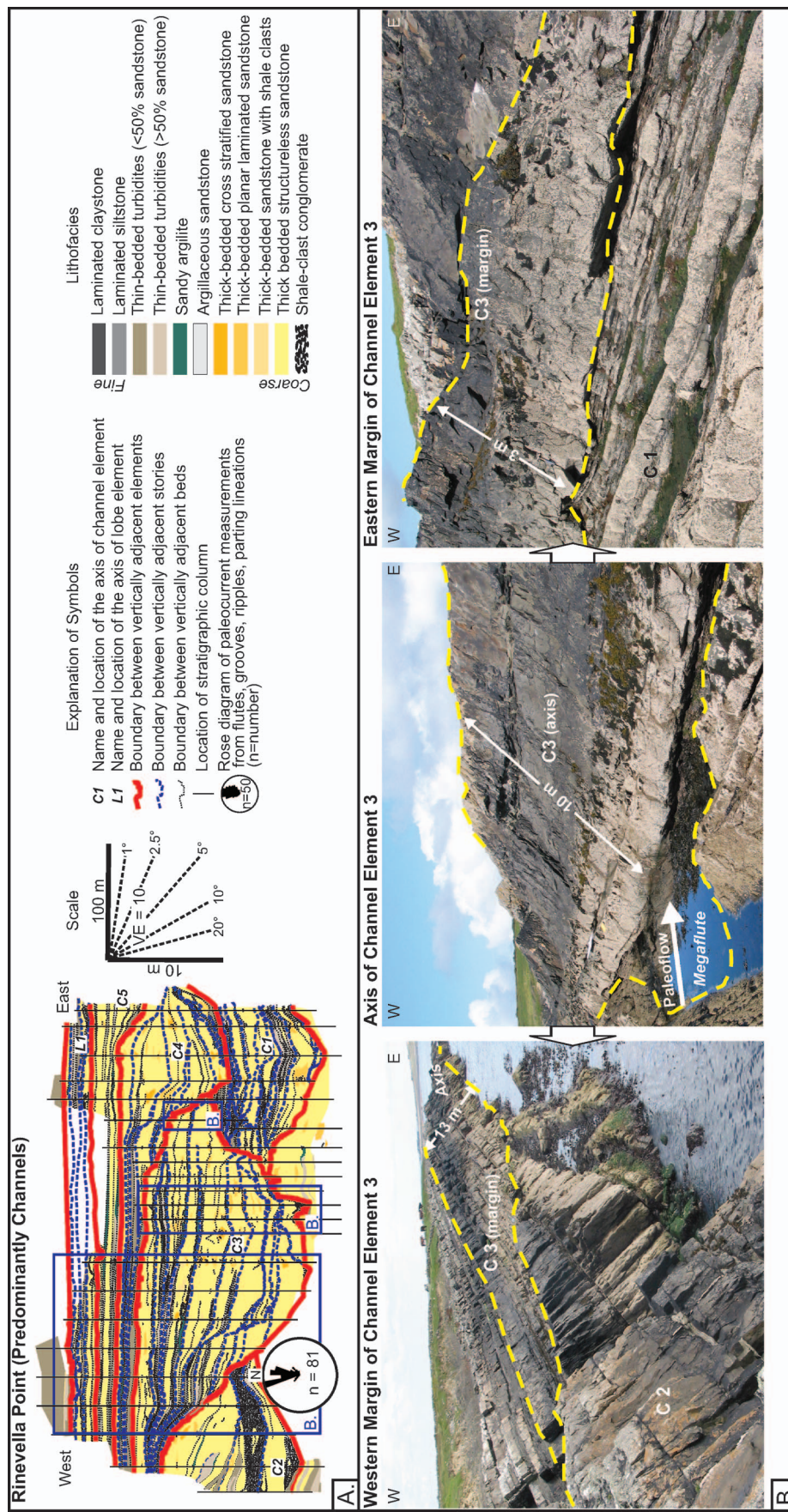


FIG. 4.—**A**) Correlation panel of the Rinnevella Point outcrop. The location of the outcrop is labeled in Figure 2. The outcrop is ~450 m wide and more than 35 m thick. Strata at this exposure dip ~30° north. The modal sediment transport direction measured from flutes, grooves, ripples, and channel-margin orientations is 350°. The outcrop is oriented normal to this direction and is therefore a strike profile through the succession. The outcrop contains five channel elements and one lobe element comprising ~95% and ~5% of the cross-sectional area of the exposure, respectively. Modified from Pyles (2004). **B**) Photographs documenting axis-to-margin and upward changes in the stratigraphy of channel element 3. The upper and lower boundaries of the element are labeled with the yellow dashed lines. Locations of photographs are labeled in Part A.

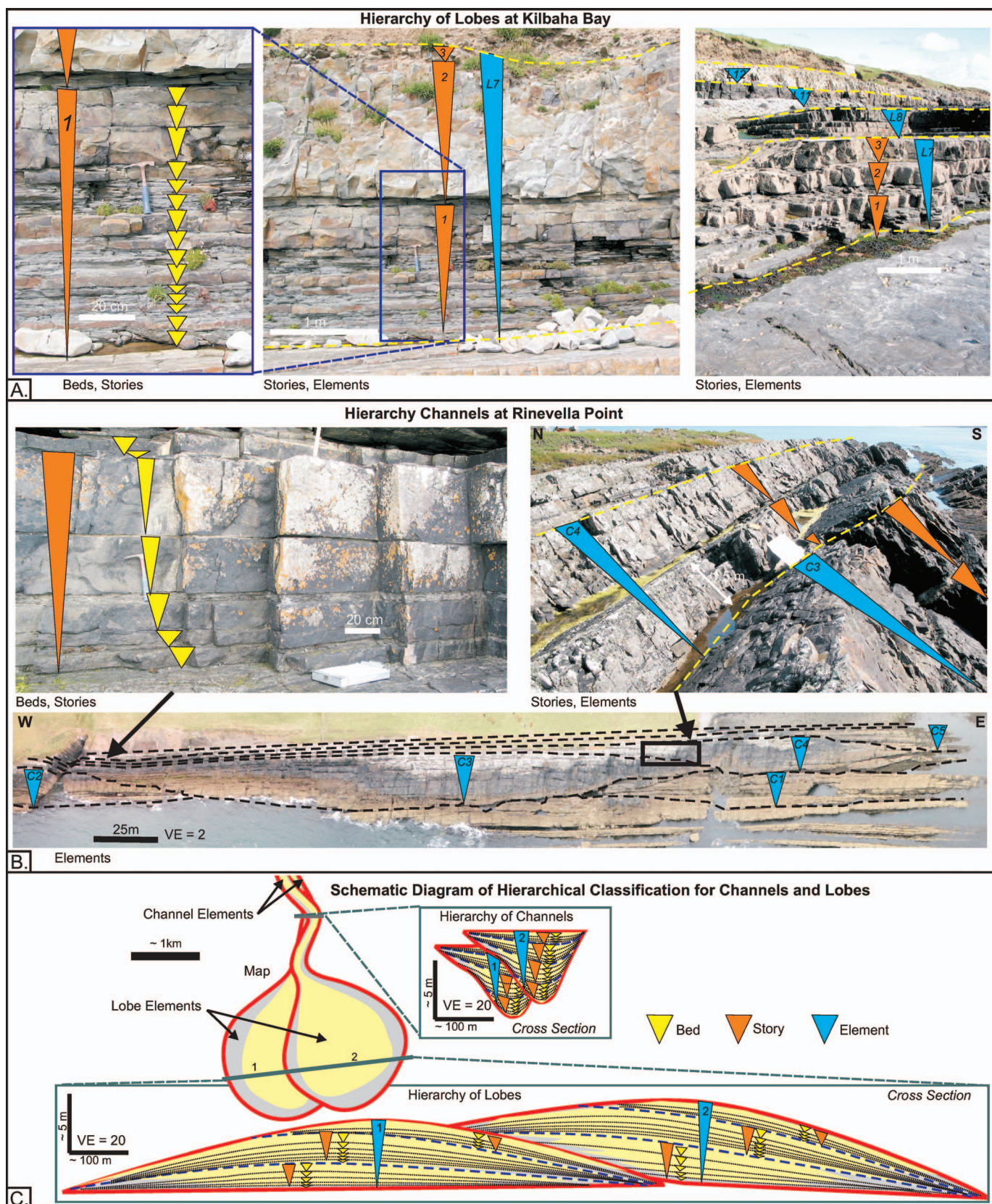


FIG. 5.—Photographic examples of beds, stories, and elements for A) lobes at Kilbaha Bay and B) channels at Rinevella Point. In both examples, beds stack to build stories and stories stack to build elements. Yellow triangles represent beds, orange triangles represent stories, blue triangle represent elements. C) Schematic diagram of the hierarchical classification used herein for channels and lobes. The diagrams are based on observations from outcrops in the Ross Sandstone. These two contrasting architectural styles are interpreted to represent proximal and distal parts of a distributive network, respectively (Sullivan et al. 2000).

TABLE 1.—Table documenting our interpretation of how hierarchical terms used in this article compare to those in selected other studies. In this study, hierarchical terms are used as modifiers to the types of architectural elements (e.g., lobe story and lobe element).

Lobes				Channels		
This study	Prelat et al. (2009, 2010)	Deptuck et al. (2008)	Macdonald et al. (2011)	This study, Pyles et al. (2007)	Gardner and Borer (2000)	Pyles et al. (2010)
N/A	Lobe Complex	Lobe Complex	N/A	N/A	Channel Conduit	N/A
Lobe Complex*	Lobe	Composite Lobe	N/A	Channel Complex*	Channel Complex	Channel Complex
Lobe Element	Lobe Element	Lobe Element	Lobe Element	Channel Element	Single-Story Channel	Channel Element
Lobe Story	N/A	N/A	N/A	Channel Story	Geobody	Channel Story
Lobe Bed	Bed-Bedset	Bed to Bed-Set	Bed	Channel Bed	Bed	Bed

*beyond the scope of this study

classes (i.e., complexes; Table 1). These hierarchical levels are not analyzed herein, because they commonly exceed the thickness of the outcrops in the Ross Sandstone.

STATISTICAL COMPARISON

To quantify the strength of compensation at each hierarchical level, for the two outcrops described above, we use a modified version of the compensation index developed by Straub et al. (2009). The compensation index, κ , is a measure of the rate of decay of the standard deviation of sedimentation divided by subsidence, σ_{ss} , between depositional horizons with increasing vertical stratigraphic averaging scale:

$$\sigma_{ss}(T) = \left(\int_L \left[\frac{r(T; x)}{\hat{r}(x)} - 1 \right]^2 dL \right)^{1/2} \quad (1)$$

where $r(T; x)$ is the local sedimentation rate measured over a stratigraphic interval T , x is a horizontal coordinate, L is the total length of the cross section analyzed, and $\hat{r}(x)$ is the local long-term sedimentation (or subsidence) rate. Straub et al. (2009) demonstrates that σ_{ss} decreases with T , following a power law trend:

$$\sigma_{ss} = aT^{-\kappa} \quad (2)$$

where a is a leading coefficient. Figure 6A diagrammatically describes how σ_{ss} diminishes with increased temporal and spatial scales. At short time scales (t_1), subsidence is small and sedimentation is local, resulting in a poor fit between sedimentation and subsidence. However, at large time scales (t_2), subsidence increases, but due to the lateral mobility of transport systems the deposit covers a larger fraction of the basin, resulting in a better fit between sedimentation and subsidence.

Whereas the thickness of sedimentation between two stratigraphic surfaces is easy to measure, quantifying the amount of subsidence that occurred over the time that separates the two surfaces is more challenging. For the basins analyzed in Straub et al. (2009) subsidence was either exactly known or inferred. Characterizing the spatial structure of subsidence between each mapped stratigraphic surface at the field sites analyzed in this study is not possible due to their short time windows of deposition relative to long-term paleo-subsidence rates (30 cm/ky:

Strogen et al. 1996). As a result we are not able to calculate compensation indices in the method outlined in Straub et al. (2009). As a proxy for σ_{ss} , we measure the coefficient of variation, CV , in deposition between two stratigraphic surfaces:

$$CV = \left(\int_L \left[\frac{\Delta\eta(x)_{A,B}}{\bar{\Delta\eta}_{A,B}} - 1 \right]^2 dL \right)^{1/2} \quad (3)$$

where $\Delta\eta(x)_{A,B}$ is the local deposit thickness between stratigraphic surfaces A and B and $\bar{\Delta\eta}_{A,B}$ is the mean deposit thickness between surfaces A and B measured over L . The coefficient of variation allows us to characterize the variability in local deposit thickness standardized as a fraction of mean thickness, thus allowing us to compare deposit stacking patterns across many thickness scales. A modified compensation index, κ_{CV} , is the exponent in the power-law decay of CV with increasing $\bar{\Delta\eta}_{A,B}$:

$$CV = a \bar{\Delta\eta}_{A,B}^{-\kappa_{CV}} \quad (4)$$

where a is a leading coefficient in the relationship. In this application κ_{CV} values of 0.0, 0.5, and 1.0 represent pure persistence in deposition trends (anti-compensational stacking), uncorrelated deposition increments, and purely compensational stacking of deposits, respectively. Unlike the formulation of κ in the study by Straub et al. (2009) the formulation of κ_{CV} in Equations 3 and 4 assumes uniform and constant subsidence rates, and as such the shape of the deposit is influenced only by the morphodynamics of the sediment routing system (Fig. 6B). For the outcrops examined in this study, where the ratio of outcrop width to basin width is relatively small (~ 0.01 – 0.03 , $\pm 5\%$ using basin dimensions from Pyles 2008), we believe that this assumption is justifiable. Figure 6 schematically documents how the decay of CV as a function of mean deposit thickness is similar to the decay of σ_{ss} as a function of time. A recent study compared the decay of σ_{ss} and CV for an experimental deposit constructed in a basin undergoing uniform and constant subsidence and documents nearly identical values for κ and κ_{CV} suggesting in such situations that CV is a good proxy for σ_{ss} (Wang et al. 2011).

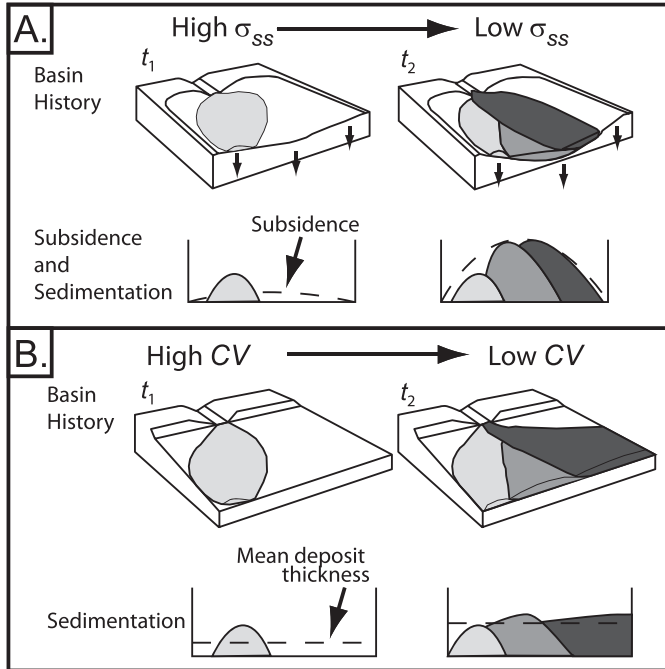


FIG. 6.—Schematic diagram modified after Lyons (2004) showing compensational stacking of lobe elements. **A)** Compensation as quantified with σ_{ss} and the balance between sedimentation and subsidence in a basin improves over time. In the block diagrams illustrating basin history, subsidence (indicated by arrows) is temporally constant but spatially variable. Sedimentation, represented by lobe elements of different color, is both temporally and spatially variable. The balance between sedimentation and subsidence for an arbitrary cross section at the two time steps is represented graphically below each block. At the earliest time, t_1 , subsidence is small and sedimentation is local, resulting in a poor fit between the two. However, through time the amount of subsidence increases and the sedimentary system occupies a larger fraction of the total area resulting, at later time t_2 , in an improved fit between sedimentation and subsidence. Taking the ratio of sedimentation over subsidence pointwise across the basin for each time step produces ratio distributions with decreasing standard deviations over time. **B)** Compensation as quantified with CV ; the sedimentation pattern through time tends to decrease in lateral variability due to reorganization of the sediment transport system to fill in topographic lows. Sedimentation, represented by lobe elements of different color, is both temporally and spatially variable. The decrease with time of depositional variability when normalized by mean deposit thickness for an arbitrary cross section at the two time steps is represented graphically below each block. At the earliest time, t_1 , mean deposit thickness is small and sedimentation is local, resulting in a poor fit between the two. However, over larger time scales mean deposit thickness increases and the sedimentary system has an opportunity to occupy a larger fraction of the total area. As a result, at time t_2 , the fit between mean deposit thickness and local deposit thickness improves at all locations in the basin. Taking the ratio of local sedimentation over mean sedimentation pointwise across the basin for each time step produces ratio distributions with decreasing CV over time.

The stratigraphic surfaces in Figures 3 and 4 are grouped into three hierarchical classes (beds, stories, elements) at each field site, resulting in six data sets. We calculate CV using measurements of $\Delta\eta(x)_{A,B}$ at horizontal increments of 0.5 m for every possible pairwise combination of surfaces in each data set, allowing us to define κ_{CV} for mean stratigraphic thicknesses of 0.05–15 m. In our analysis we include only surfaces with widths > 50 m because this produces a statistically significant number of thickness measurements to characterize CV for a pair of surfaces. Further, we calculate only CV for pairs of bed surfaces bounded between successive story boundaries and for pairs of story surfaces bounded between successive element boundaries. Finally, we note that compensation can occur at larger hierarchical scales (i.e., complexes), but this scale

is not captured in our analysis. Figure 7 shows CV scaled against mean interval thickness for the six populations. All populations contain a log-log linear decay of CV with increasing $\Delta\eta_{A,B}$ which is used to calculate κ_{CV} for each population. For the Kilbaha Bay outcrop, we measured κ_{CV} values of 0.49, 0.87, and 1.01 for beds, stories, and elements, respectively. For the Rinevella Point outcrop, we measured κ_{CV} values of 0.43, 0.68, and 0.81 for beds, stories, and elements, respectively.

To assess the differences in κ_{CV} between each population, we calculate error associated with data regression. Mean κ_{CV} and associated errors are determined by bootstrapping analysis (Efron 1979). Reported error values represent 95th percentile confidence levels for each dataset (Fig 7). Error analysis documents statistically significant differences between calculated κ_{CV} values for each population.

DISCUSSION

Data shown in Figure 7 documents that strength of compensation increases with hierarchical level in both the Kilbaha Bay (predominantly lobe elements) and Rinevella Point (predominantly channel elements) outcrops. These observations quantitatively document the strength of compensation to increase with hierarchical levels interpreted in the outcrops. If compensation were fractal, beds, stories, and elements would share similar κ_{CV} values as small- (beds) and large-scale (elements) units would stack similarly (Fig. 1). We hypothesize that punctuated shifts in κ_{CV} between hierarchical levels result from scalar differences in various allogeic forcings and autogenic processes, which are set by inherent scales of the transport system (Einsle et al. 1991; Hoyal and Sheets 2009). We propose that bed-scale stacking in channel elements is influenced by the size of flows and the width of the channel whereas bed-scale stacking in lobe elements is influenced by focusing from the updip, genetically related channel, meaning that while lobes have no lateral boundary condition (i.e., channel walls) the location of the sediment transport field is laterally constrained, or focused, by the fixed updip channel that feeds sediment to the lobe element. Furthermore, we propose that larger, element-scale stacking results from processes such as avulsion, which have longer time and space scales, and are possibly influenced by different morphodynamic properties of the system. These properties could include allogeic forcings such as frequency of flow events, long-term sediment supply, subsidence rate, and the size and shape of the basin and/or autogenic processes including superelevation and the development of lateral slopes of the channel-lobe element due to sedimentation (Straub and Mohrig 2008; Prelat et al. 2010; Macdonald et al. 2011). These scale-dependent dynamics are imprinted in the stratigraphic record and quantitatively manifested as the punctuated shifts in κ_{CV} with scale (Fig. 7). The increase in κ_{CV} with hierarchical scale also indicates an increase in stratigraphic organization with scale as κ_{CV} values near 0.5 indicate random stacking patterns, while κ_{CV} values near 1.0 represent organized stacking of deposits with pure compensation (Straub et al. 2009).

Indeed some aspects of stratigraphy, such as shape of clinoforms (Schlager 2004), are fractal or scale invariant; however, other aspects, such as compensation, are hierarchical. Therefore grouping stratigraphy into hierarchical units sometimes captures natural structure and is not necessarily a subdivision of convenience.

Furthermore, our analysis documents that strata at Kilbaha Bay (predominantly lobe elements) stack more compensationally than strata at Rinevella Point (predominantly channel elements) for each hierarchical level (Fig. 7). This pattern is interpreted to result from the enhanced mobility of unconfined lobe elements relative to their channel-element counterparts. Beds and associated gravity currents in channels are laterally confined by the walls of the channel, whereas beds associated with gravity currents in lobes have little-to-no lateral confinement, allowing them to spatially expand, thereby responding more easily to

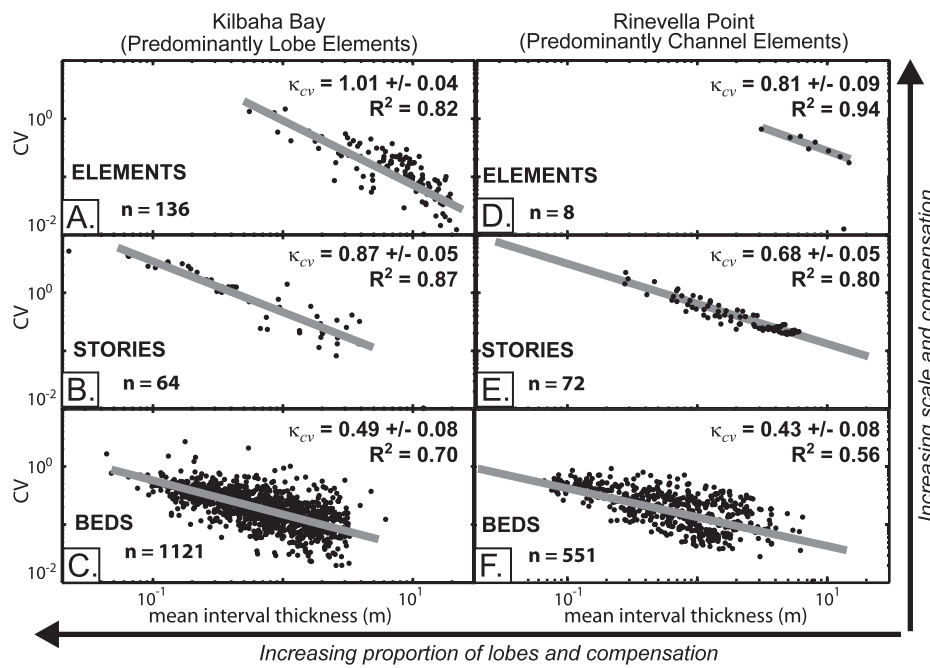


FIG. 7.—Decay of CV with increasing $\Delta\eta_{A,B}$ for beds, stories, and elements of the A–C) Kilbaha Bay and D–F) Rinevella Point outcrops. Number of data points, n , used in κ_{CV} regression and error is presented for each. At both the Kilbaha Bay and Rinevella Point, κ_{CV} increases through the hierarchical levels. Furthermore κ_{CV} is higher in lobe elements (Kilbaha Bay) than channel elements (Rinevella Point).

lateral slopes developed by depositional trends, despite focusing by the genetically related updip channel. Additionally, this pattern is interpreted to demonstrate that compensation varies spatially in distributive settings. Sullivan et al. (2000) interprets the contrasting architectural styles between Rinevella Point (predominantly channel elements) and Kilbaha Bay (predominantly lobe elements) to reflect proximal and medial parts of a distributive submarine network, respectively (Fig. 5C). It is plausible that the differences in compensation between these two data sets reflect that compensation increases along a longitudinal transect through this distributive submarine fan.

APPLICATIONS

This study provides justification for using hierarchical frameworks for characterizing some aspects of stratigraphic systems. Results can be used to constrain rules for event-based stratigraphic models (e.g., Pyrcz et al. 2005), whereby sedimentation is dictated by empirically defined patterns, such as compensation. These models can be used by the oil and gas industry for making production forecasts through fluid-flow simulations.

The documented patterns also have applications to the oil and gas industry by improving one's ability to predict static connectivity in deepwater reservoirs. In an effort to relate stratigraphic architecture described in outcrops to reservoir characteristics, Funk et al. (2012) defined two metrics for static connectivity: (1) margin connectivity and (2) sand-on-sand connectivity. Margin connectivity (C_m) is the fractional length between two stratigraphically adjacent elements not obstructed by a barrier. Sand-on-sand connectivity (C_s) is the fractional length of sand-on-sand contacts between two stratigraphically adjacent elements. Figure 1 shows diagrammatic examples of hierarchical and fractal compensation. The two stacking patterns result in fundamentally different static connectivity. Figure 1A shows smaller units to stack vertically, or anti-compensationally, whereas larger units are shown to stack more compensationally—a hierarchical pattern similar to that documented herein (Fig. 7). In this example static connectivity is relatively high in small units and relatively low in large units. In contrast, Figure 1B shows small units and large units to stack equally compensationally, a fractal pattern, resulting in low static connectivity at all scales.

CONCLUSIONS

This article demonstrates that subdivision of stratigraphy into hierarchical units (e.g., beds, stories, elements) through field observations results in groupings with quantitatively different degrees of compensation. These results are interpreted to document that: (1) hierarchical divisions based on compensation are justified, and (2) compensation increases along a longitudinal transect through this distributive submarine fan. We recommend future studies to: (1) use this approach to test compensation in more submarine-fan deposits, (2) test if this concept translates to fluvial and deltaic strata, (3) examine how the strength of compensation varies in the third dimension, (4) use quantitative analyses to determine which characteristics of the stratigraphic record are hierarchical and which are fractal. Results from this study and others like it will significantly improve our ability to make predictions of stratigraphic architecture, thereby reducing uncertainty in the exploration and production of resources from sedimentary systems.

ACKNOWLEDGMENTS

Financial support for DRP was provided by Chevron to the Chevron Center of Research Excellence at the Colorado School of Mines. KMS received support from National Science Foundation grant EAR-1024443. We thank L. Martin for gridding outcrop surfaces into data sets for use in the statistical analyses. Bryan Cronin, Andrew Petter, Jeff Peakall, and Brian Romans are thanked for constructive reviews that greatly improved this manuscript.

REFERENCES

- BROWN, L.F., AND FISHER, W.L., 1977, Seismic-stratigraphic interpretation of depositional systems: examples from the Brazilian rift and pull-apart basins, in Payton, C.E., ed., *Seismic Stratigraphy—Applications to Hydrocarbon Exploration*: American Association of Petroleum Geologists, Memoir 26, p. 7–26.
- CAMPBELL, C.V., 1967, Lamina, laminaset, bed, bedset: *Sedimentology*, v. 8, p. 7–26.
- CHAPIN, M.A., DAVIES, P., GIBSON, J., AND PETTINGILL, H.S., 1994, Reservoir architecture of turbidite sheet sandstones in laterally extensive outcrops, Ross Formation, western Ireland, in Weimer, P., Bouma, A.H., and Perkins, B.F., eds., *Submarine Fans and Turbidite Systems: Sequence Stratigraphy, Reservoir Architecture, and Production Characteristics: Gulf Coast Section*, SEPM, 15th Annual Research Conference, p. 53–68.

- COLLINSON, J., MARTINSEN, O.J., BAKKEN, B., AND KLOSTER, A., 1991, Early fill of the western Irish Namurian basin: a complex relationship between turbidites and deltas: *Basin Research*, v. 3, p. 223–242.
- DARWIN, C., 1861, *On the Origin of Species by Means of Natural Selection, or the Preservation of Favoured Races in the Struggle for Life* (Third Edition): London, John Murray, 538 p.
- DEPTUCK, M.É., PIPER, D.J.W., SAVOYE, B., AND GERVais, A., 2008, Dimensions and architecture of late Pleistocene submarine lobes off the northern margin of East Corsica: *Sedimentology*, v. 55, p. 869–898.
- EFRON, B., 1979, Bootstrap methods: another look at the jackknife: *The Annals of Statistics*, v. 7, p. 1–26.
- EINSELE, G., RICKEN, W., AND SEILACHER, A., 1991, *Cycles and Events in Stratigraphy*: Berlin, Springer-Verlag, 1040 p.
- ELLIOTT, T., 2000, Depositional architecture of a sand-rich, channelized turbidite system: the upper Carboniferous Ross Sandstone Formation, western Ireland, *in* Weimer, P., Slatt, R.M., Coleman, J.M., Rossen, N.C., Nelson, H., Bouma, A.H., Styzen, M.J., and Lawrence, D.T., eds., *Deep-water reservoirs of the world: Gulf Coast Section SEPM, 15th Annual Research Conference*, p. 342–373.
- FRIEND, P.F., SLATER, M.J., AND WILLIAMS, R.C., 1979, Vertical and lateral building of river sandstone bodies, Ebro Basin, Spain: *Geological Society of London, Journal*, v. 136, p. 39–46.
- FUNK, J.E., SLATT, R.M., AND PYLES, D.R., 2012, Quantification of static connectivity between deep-water channels and stratigraphically adjacent architectural elements using outcrop analogs: *American Association of Petroleum Geologists, Bulletin*, v. 96, p. 277–300.
- GARDNER, M.H., AND BORER, J.M., 2000, Submarine channel architecture along a slope to basin profile, Brushy Canyon Formation, west Texas, *in* Bouma, A., and Stone, C.G., eds., *Fine-Grained Turbidite Systems*: American Association of Petroleum Geologist Memoir 72/SEPM Special Publication 68, p. 195–214.
- GHIBAUDO, G., 1980, Deep-sea fan deposits in the Macigno Formation (Middle–Upper Oligocene) of the Gordano Valley, Northern Apennines, Italy: *Journal of Sedimentary Petrology*, v. 50, p. 723–742.
- HOYAL, D.C.J.D., AND SHEETS, B.A., 2009, Morphodynamic evolution of experimental cohesive deltas: *Journal of Geophysical Research, Earth Surface*, v. 114, p. F02009, doi:10.1029/2007JF000882.
- JACKSON, R.G., 1975, Hierarchical attributes and a unifying model of bed forms composed of cohesionless material and produced by shearing flow: *Geological Society of America, Bulletin*, v. 86, p. 1523–1533.
- LIEN, T., WALKER, R.G., AND MARTINSEN, O.J., 2003, Turbidities in the Upper Carboniferous Ross Formation, western Ireland: reconstructions of a channel and spillover system: *Sedimentology*, v. 50, p. 113–148.
- LYONS, W.J., 2004, *Quantifying Channelized Submarine Depositional Systems from Bed to Basin Scale* [Ph.D. thesis]: Cambridge, Massachusetts Institute of Technology, 252 p.
- MACDONALD, H.A., PEAKALL, J., WIGNALL, P.B., AND BEST, J., 2011, Sedimentation in deep-sea lobe-elements: implications for the origin of thickening-upward sequences: *Geological Society of London, Journal*, v. 168, p. 319–331.
- MARTINSEN, O.J., LIEN, T., AND WALKER, R.G., 2000, Upper Carboniferous deep water sediments, western Ireland: analogues for passive margin turbidite plays, *in* Weimer, P., Slatt, R.M., Coleman, J.M., Rossen, N.C., Nelson, H., Bouma, A.H., Styzen, M.J., and Lawrence, D.T., eds., *Deep-Water Reservoirs of the World*, Gulf Coast Section SEPM, 15th Annual Research Conference, p. 533–555.
- MARTINSEN, O.J., LIEN, T., WALKER, R.G., AND COLLINSON, J.D., 2003, Facies and sequential organisation of a mudstone-dominated slope and basin floor succession: the Gull Island Formation, Shannon Basin, Western Ireland: *Marine and Petroleum Geology*, v. 20, p. 789–807.
- MASLOW, A.H., 1943, A theory of human motivation: *Psychology Review*, v. 50, p. 370–396.
- MITCHUM, R.M., VAIL, P.R., AND SANGREE, J.B., 1976, Seismic stratigraphy and global changes of sea-level, part 6: stratigraphic interpretation of seismic reflection patterns in depositional sequences, *in* C.E. Payton, ed., *Seismic Stratigraphy—Applications to Hydrocarbon Exploration*: American Association of Petroleum Geologists, Memoir 26, p. 117–163.
- MUTTI, E., AND NORMARK, W.R., 1987, Comparing examples of modern and ancient turbidite systems: problems and concepts, *in* Leggett, J.K., and Zuffa, G.G., eds., *Marine Clastic Sedimentology; Concepts and Case Studies*: London, Graham and Trotman, p. 1–38.
- MUTTI, E., AND SONNINO, M., 1981, Compensational cycles: a diagnostic feature of turbidite sandstone lobes [abstract]: International Association of Sedimentologists, Second European Regional Meeting, p. 120–123.
- NORMARK, W.R., PIPER, D.J.W., AND HESS, G.R., 1979, Distributary channels, sand lobes and mesotopography of Navy submarine fan, California Borderland, with applications to ancient fan sediments: *Sedimentology*, v. 26, p. 749–774.
- PEAKALL, J., McCAFFREY, B., AND KNELLER, B., 2000, A process model for the evolution, morphology, and architecture of sinuous submarine channels: *Journal of Sedimentary Research*, v. 70, p. 434–448.
- PRAETHER, B.E., KELLER, F.B., AND CHAPIN, M.A., 2000, Hierarchy of deep-water architectural elements with reference to seismic resolution: implications for reservoir prediction and modeling: *Gulf Coast Section, SEPM Foundation, 20th Annual Research Conference, Deep-Water Reservoirs of the World*, p. 817–835.
- PRELAT, A., HODGSON, D.M., AND FLINT, S.S., 2009, Evolution, architecture and hierarchy of distributary deep-water deposits: a high-resolution outcrop investigation from the Permian Karoo Basin, South Africa: *Sedimentology*, v. 56, p. 2132–2154.
- PRELAT, A., COVIAULT, J.A., HODGSON, D.M., FILDANI, A., AND FLINT, S.S., 2010, Intrinsic controls on the range of volumes, morphologies, and dimensions of submarine lobes: *Sedimentary Geology*, v. 232, p. 66–76.
- PYLES, D.R., 2004, *On the Stratigraphic Evolution of a Structurally Confined Submarine Fan, Carboniferous Ross Sandstone, Western Ireland* [Ph.D. thesis]: Boulder, University of Colorado, 322 p.
- PYLES, D.R., 2007, Architectural elements in a ponded submarine fan, Carboniferous Ross Sandstone, western Ireland, *in* Nilsen, T.H., Shew, R.D., Steffens, G.S., and Studlick, J.R.J., eds., *Atlas of Deep-Water Outcrops*: American Association of Petroleum Geologists, *Studies in Geology* 56, CD-ROM, p. 19.
- PYLES, D.R., 2008, Multiscale stratigraphic analysis of a structurally confined submarine fan: Carboniferous Ross Sandstone, Ireland: *American Association of Petroleum Geologists, Bulletin*, v. 92, p. 557–587.
- PYLES, D.R., AND JENNETTE, D.C., 2009, Geometry and architectural associations of co-genetic debrite–turbidite beds in basin-margin strata, Carboniferous Ross Sandstone (Ireland): applications to reservoirs located on the margins of structurally confined submarine fans: *Marine and Petroleum Geology*, v. 26, p. 1974–1996.
- PYLES, D.R., JENNETTE, D.C., TOMASSO, M., BEAUBOEUF, R.T., AND ROSSEN, C., 2010, Concepts learned from a 3d outcrop of a sinuous slope channel complex: Beacon Channel Complex, Brushy Canyon Formation, West Texas, U.S.A.: *Journal of Sedimentary Research*, v. 80, p. 67–96.
- PYLES, D.R., SYVITSKI, J.P.M., AND SLATT, R.M., 2011, Defining the concept of stratigraphic grade and applying it to stratal (reservoir) architecture and evolution of the slope-to-basin profile: an outcrop perspective: *Marine and Petroleum Geology*, v. 28, p. 675–697.
- PYRCZ, M.J., CATUNEAU, O., AND DEUTSCH, C.V., 2005, Stochastic surface-based modeling of turbidite lobes: *American Association of Petroleum Geologists, Bulletin*, v. 89, p. 177–191.
- RIDER, M.H., 1974, The Namurian of west County Clare: *Royal Irish Academy Proceedings*, v. 74b, p. 125–142.
- SAGEMAN, B.B., GARDNER, M.H., ARMENTROUT, J.M., AND MURPHY, A.E., 1998, Stratigraphic hierarchy of organic carbon-rich siltstones in deep-water facies, Brushy Canyon Formation (Guadalupe), Delaware Basin, west Texas: *Geology*, v. 26, p. 451–454.
- SCHLAGER, W., 2004, Fractal nature of stratigraphic sequences: *Geology*, v. 32, p. 185–188.
- SCHLAGER, W., 2010, Ordered hierarchy versus scale invariance in sequence stratigraphy: *International Journal of Earth Sciences*, v. 99, p. S139–S151.
- STOW, D.A.V., AND JOHANSSON, M., 2000, Deep-water massive sands: nature, origin and hydrocarbon implications: *Marine and Petroleum Geology*, v. 17, p. 145–174.
- STRAUB, K.M., AND MOHRIG, D., 2008, Quantifying the morphology and growth of levees in aggrading submarine channels: *Journal of Geophysical Research, Earth Surface*, v. 113, p. F03012, doi:10.1029/2007JF000896.
- STRAUB, K.M., PAOLA, C., MOHRIG, D., WOLINSKY, M.A., AND GEORGE, T., 2009, Compensational stacking of channelized sedimentary deposits: *Journal of Sedimentary Research*, v. 79, p. 673–688.
- STROGEN, P., SOMERVILLE, I.D., PICKARD, N.A.H., JONES, G., AND FLEMING, M., 1996, Controls on ramp, platform, and basinal sedimentation in the Dinantian of the Dublin Basin and Shannon trough, Ireland, *in* Strogen, P., Somerville, I.D., and Jones, G., eds., *Recent Advances in Lower Carboniferous Geology*: Geological Society of London, Special Publication 107, p. 263–279.
- SULLIVAN, M.D., JENSEN, G.N., GOULDING, F., JENNETTE, D.C., FOREMAN, J.L., AND STERN, D., 2000, Architectural analysis of deep-water outcrops: implications for exploration and development of the Diana sub-basin, Western Gulf of Mexico: *Gulf Coast Section, SEPM Foundation, 20th Annual Research Conference: Deep-Water Reservoirs of the World*, p. 1010–1031.
- WANG, Y., STRAUB, K.M., AND HAJEK, E.A., 2011, Scale-dependent compensational stacking: an estimate of autogenic time scales in channelized sedimentary deposits: *Geology*, v. 39, p. 811–814.
- WEIMER, P., AND LINK, M.H., 1991, *Seismic Facies and Sedimentary Process of Submarine Fans of Submarine Systems*: New York, Springer-Verlag, p. 9–67.
- WIGNALL, P.B., AND BEST, J.L., 2000, The Western Irish Namurian Basin reassessed: *Basin Research*, v. 12, p. 59–78.

Received 11 August 2011; accepted 18 September 2012.